

Effect of martensitic transformation and magnetic field on transport properties of Ni-Mn-Ga and Ni-Fe-Ga Heusler alloys

J. M. Barandiarán,^{1,*} V. A. Chernenko,^{1,2} P. Lázpita,¹ J. Gutiérrez,¹ and J. Feuchtwanger¹
¹*Departamento de Electricidad y Electrónica, Universidad del País Vasco, P.O. Box 644, E-48080 Bilbao, Spain*
²*IKERBASQUE, Basque Foundation for Science, 48011 Bilbao, Spain*

(Received 26 March 2009; revised manuscript received 3 August 2009; published 4 September 2009)

We study the magnetic-field influence on the martensitic transformation temperatures and the accompanying anomaly in the resistivity by extensive measurements of the temperature dependencies of resistivity of several Ni-Mn-Ga and Ni-Fe-Ga alloys. A low-field minimum of the martensitic transformation temperature versus magnetic-field curves is observed for single and polycrystalline Ni-Mn-Ga alloys. This minimum is confirmed by magnetization loop measurements showing a magnetic anisotropy contribution to the ordinary Clausius-Clapeyron relationship which describes the martensitic transformation. This minimum did not appear for Ni-Fe-Ga polycrystalline alloys because in this case the difference in the magnetic anisotropy of relevant phases is small. We did not find any systematic behavior of the magnetoresistance related to the phase in which it is measured. In the vicinity of the martensitic transformation, the magnetoresistance exhibits a peaklike behavior which is explained in terms of the combined influence of the zero-field resistivity anomaly at the transition and the magnetic-field-induced shift of the transformation temperature.

DOI: [10.1103/PhysRevB.80.104404](https://doi.org/10.1103/PhysRevB.80.104404)

PACS number(s): 75.50.Cc, 65.40.Ba, 75.30.Gw, 75.80.+q

I. INTRODUCTION

A number of the ferromagnetic intermetallics, such as X_2YZ Heusler compounds ($X=3d$ metal, $Y=Mn$, other $3d$ metal, or rare earth, Z =element from group III or IV of the Periodic Table) as well as Fe_3Pt and $Fe-Pd$ alloys exhibit a thermoelastic martensitic transformation (MT). Some of these alloys also show premartensitic and intermartensitic transitions. Alongside the conventional shape memory effect (SME) (e.g., Ref. 1), ferromagnetic martensites also show the ferromagnetic shape memory effect (FSME) (e.g., Ref. 2). SME is due to the reverse MT and consists of a thermally activated shape recovery when the austenite phase is reached, after having been mechanically deformed in the martensitic state. FSME, instead, consists of a magnetic-field-induced twin rearrangement within the martensitic phase, whereby an equivalent strain is reversibly generated by the magnetic field oriented along the hard magnetic direction of the twin variant. Modulated tetragonal or orthorhombic Ni-Mn-Ga martensites are the prototypical FSME alloys (FSMAs) and show cycling magnetic-field-induced strains up to 10%. The modulation of the martensitic lattice consists of atomic displacements propagating along the $[110]$ direction with $[1\bar{1}0]$ polarization^{3,4} and a typical periodicity of 10 or 14 interatomic distances. These structures are named 10 M or 14 M, respectively. The martensitic phases in Ni-Fe-Ga alloys also show modulated structures.⁵⁻⁷ The latter alloys are increasingly attracting attention due to their appreciable ductility.

The MT in FSMAs greatly influences their transport properties. Particularly the resistivity in Ni-Mn-Ga alloys exhibits a large jumplike anomaly at the transformation temperature T_M . The magnitude of the jump depends on the value of T_M and ranges from less than 1% to about 20% for $T_M \approx 180$ (Ref. 8) and 400 K,⁹ respectively. In the case of ternary Ni-Fe-Ga alloys, these anomalies were found to be about 25% and 30% for $T_M \approx 140$ (Ref. 5) and 250 K,¹⁰ respectively.

The influence of magnetic fields up to 9 T on the resistivity, either in the vicinity of MT or in an extended temperature range, has been examined for Ni-Mn-Ga alloys in a limited number of publications,¹¹⁻¹⁵ whereas similar studies have not been yet reported for Ni-Fe-Ga alloys. An almost linear negative magnetoresistance, $MR(\%) = 100[R(H) - R(0)]/R(0)$, has been obtained in all phases of bulk polycrystalline $Ni_{2+x}Mn_{1-x}Ga$ alloys, with maximum values of about -5% at room temperature.¹³ In contrast, the MR results for melt-spun Ni-Mn-Ga ribbon reveal both a nonlinear behavior and maxima about -10% at T_M .¹² Sputter-deposited Ni-Mn-Ga thin films show diverse MR dependencies when recorded at different temperatures. Maximum values are about -5% at 5 K.¹¹ Different mechanisms have been suggested to account for these MR observations but most explanations remain obscure and controversial.¹¹⁻¹³

Another fundamental aspect of the resistivity studies under magnetic field in the vicinity of MT is the possibility of being used as a direct determination of the magnetic-field shift of the transformation temperature. Resistivity measurement can be considered a simpler and more reliable method than others used so far, e.g., magnetization,¹⁶⁻²⁰ strain,²¹ or x-ray diffraction²² methods. Note, for instance, that the thermomagnetization curve often does not show pronounced anomaly at T_M to be precisely monitored under magnetic field (e.g., Ref. 15). Some results on the influence of the magnetic field on T_M and T_1 (where T_1 is the premartensitic transition temperature) in near stoichiometric Ni_2MnGa alloys are available in the literature though they are contradictory (e.g., cf. Ref. 14 and Refs. 16 and 22). However, this influence has scarcely been addressed for other FSMAs, including Ni-Fe-Ga alloys.

In this paper, we intend to clarify the influence of the magnetic field on the structural transition temperatures and magnetoresistance of the martensitic and austenitic phases of the ferromagnetic shape memory alloys. Systematic and pre-

cise measurements of the relative resistivity as a function of temperature and magnetic field have been carried out in two quasistoichiometric Ni₂MnGa alloys (in single crystal and polycrystalline form) and three polycrystalline Ni-Fe-Ga alloys. Temperatures ranging from 100 to 300 K and magnetic field up to 14 T have been used. The selection of the alloys aims to address the magnetic anisotropy and composition effects. A phenomenological approach is used for the analysis of the results. This analysis will provide a comparison of the magnetoresistance and magnetic-field dependence of the structural transitions in Heusler alloys with quite different physical properties but similar transition temperatures, so that the relative importance of the different mechanisms involved in the mentioned processes can be better understood.

II. EXPERIMENTAL PROCEDURE

One single crystal Ni_{49.5}Mn_{25.4}Ga_{25.1} (Ni49SC) and one polycrystalline Ni_{51.1}Mn_{24.9}Ga_{24.0} (Ni51PC) alloy ingot as well as three polycrystalline alloys with compositions Ni_{55-x}Fe_{19+x}Ga₂₆ [$x=0$ (Fe19PC), $x=1$ (Fe20PC), and $x=2$ (Fe21PC)] have been used for this work. Ingots of Ni-Mn-Ga alloys were prepared by induction melting under argon atmosphere and cast into a copper mold. Further details of ingot fabrication are given elsewhere.^{7,10,23,24} The single crystal Ni49SC was grown by the Bridgman method. Ni-Fe-Ga alloys were prepared by arc melting, then homogenized at 1353 K for 24 h, and quenched into water. They were subsequently annealed at 973 K for 7 h and cooled slowly to room temperature to stabilize the $L2_1$ austenitic phases. These Ni-Fe-Ga alloys have been shown to contain a disordered fcc γ phase with a volume fraction up to 18%.^{7,10} The transition temperatures and the structure of the martensitic phases have previously been investigated by x-ray, neutron, Mössbauer, and also differential scanning calorimetry and magnetic measurements.^{7,10,24–27} According in Refs. 7, 10, and 24–27, the Ni-Mn-Ga alloys exhibit, during cooling, a soft-mode-condensed premartensitic transition to a cubic I phase and then another transition to a tetragonal 10 M martensite. Fe-containing alloys exhibit only a direct transition to an orthorhombic 14 M martensite.

Precise measurements of the relative change in electrical resistivity as a function of temperature and/or magnetic field were carried out by four-probe measurements in a measuring platform from Cryogenic Ltd., in fields up to 14 T. The samples were cut into rectangular prisms of $1.0 \times 1.0 \times 10$ mm³. In the case of single crystal, the prism was of $0.4 \times 1.0 \times 10$ mm³. Silver paste was used to make the electrical contacts. The magnetic field was applied parallel to the measuring electrical current and the resistance was obtained by averaging the forward and reverse voltage drops at the sample. Accuracy in the absolute resistivity values was about 5% due to geometrical uncertainty in the samples, while repeatability was better than 0.02% in different runs of the same sample. A magnetic-field change rate of 0.25 T/min was used during isothermal measurements. The temperature was determined using a cermet temperature sensor (Lake-shore Cernox CX 1030 thermometer) with an accuracy better than 0.01 K. The cooling-heating ramps were performed at a

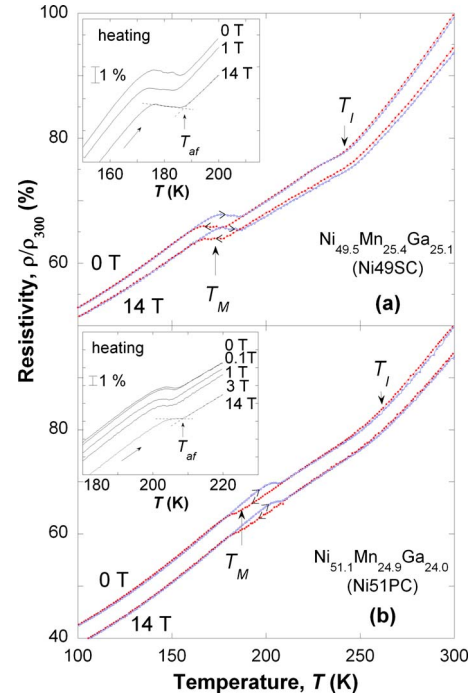


FIG. 1. (Color online) Typical temperature dependencies of resistivity recorded at constant magnetic fields for the Ni-Mn-Ga single crystalline (Ni49SC) (a) and polycrystalline (Ni51PC) (b) alloys, showing anomalies produced by the transformation between parent phase (p) and the premartensitic phase (i) at T_I and between the I phase and martensitic phase at T_M . The austenite finish temperature T_{af} is determined by a tangential method. Insets are zooms showing the influence of the magnetic field on the heating curves in the vicinity of the martensitic transformation.

rate of 1 K/min. The sample holder design assured its thermal stability better than 5×10^{-3} K.

Magnetization loops and thermomagnetization curves were obtained by a superconducting quantum interference device magnetometer (Quantum Design MPMS-7).

III. RESULTS AND DISCUSSION

In the following, we show that the extensive measurements of the temperature dependence of resistivity under different constant magnetic fields made possible a self-consistent analysis of both the influence of magnetic field on the structural transformation characteristics and the behavior of magnetoresistance as a function of temperature, magnetic field, and structural state.

A. Resistivity changes at the transformation temperatures

Figures 1 and 2 depict two cooling and heating resistivity curves, $\rho(T)$, measured for the alloys studied under no field and 14 T. Data for Fe20PC and Fe21PC are not shown due to the qualitative similarity to the Fe19PC alloy. Resistivity curves obtained at intermediate magnetic fields between those indicated show a continuous downward shift as a function of field. Several typical heating branches of the resistivity in the vicinity of the MT are shown in the insets of Figs.

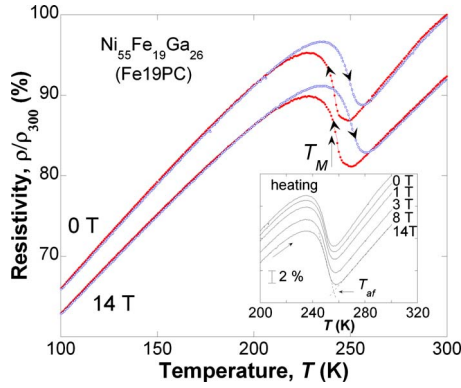


FIG. 2. (Color online) Selected resistivity curves of a sample Fe19PC under magnetic field, typical for the studied Ni-Fe-Ga alloys. Inset is a detailed view of heating curves in the vicinity of martensitic transformation. Symbols are the same as in Fig. 1.

1 and 2. In the alloys studied, the resistivity exhibits a hysteretic anomaly at MT which is typical for the ferromagnetic Heusler alloys transforming martensitically (e.g., Ref. 8, 17, and 28). Ni-Fe-Ga alloys show only the martensitic transition, whereas the Ni-Mn-Ga alloys additionally display a low-hysteretic premartensitic transformation into a micro-modulated intermediate phase at T_I . As explained in many works, the latter transition is attributed to the freezing of a soft phonon mode^{3,4,29} which occurs regardless of whether the subsequent martensitic transformation takes place or not.³⁰ The resistivity change at MT is much larger for the Fe-based compounds that undergo a phase transition directly from the nonmodulated cubic phase to the layered martensitic phase so that the disorder induced in the transition is much larger than in Ni-Mn-Ga alloys that transform martensitically from the already micro-modulated soft-mode condensed cubic phase. The values of the structural transition temperatures at zero magnetic field, measured in the present work, are shown in Table I and are in agreement with previous results.^{7,10,24–27}

In Heusler alloys, and not too close to 0 K, two main contributions to $\rho(T)$ have been considered:²⁸ the lattice contribution, caused by the electron-phonon scattering, $\rho_{\text{el-ph}}(T)$, and the magnetic contribution, due to electron-magnon scattering, $\rho_{\text{el-m}}(T)$. Each of those mechanisms has a different temperature variation. There is also a temperature-

independent contribution, the residual resistivity, ρ_0 , originated at the lattice defects and chemical disorder.

However, a rigorous analysis of the resistivity curves of Ni-Mn-Ga, such as model calculations in Ref. 28, cannot be taken as conclusive. Particularly, it does not provide an explanation of the experimentally observed $\rho(T)$ anomalies at the phase transformations. We believe that this failure is due to the underestimation of the role of the residual resistivity. The following simple arguments can emphasize its relevance.

Changes in both the $\rho_{\text{el-ph}}(T)$ and $\rho_{\text{el-m}}(T)$ can contribute to the resistivity anomalies at the martensitic and premartensitic transformations. According to the well-known Bloch-Grüneisen function, $\rho_{\text{el-ph}}$ is only affected by changes in the Debye temperature, θ_D . From elastic modulus and specific heat measurements (see Refs. 24 and 31 and references therein) one can deduce that the θ_D of the martensite is larger than that of the austenite. The difference, however, is very small and differs in the sign of the observed resistivity anomaly. The magnon-phonon scattering depends on both the magnetic moment and the Curie temperature, which have only slight differences between the different phases of the same alloy (see Refs. 32 and 33). Since all mentioned effects are small, ρ_0 , related to the static disorder, must play an important role. The modulated and low-symmetry phases are expected to have a larger residual resistivity and lower thermal coefficient of resistivity than the cubic austenite, much like in amorphous alloys. Therefore, in our opinion, the main term affecting the resistivity at the transition is the change in residual resistivity that accompanies the increase in static disorder. If the disorder in the structure develops continuously, as is the case at T_I , the transition manifests itself as a change in the resistivity slope and since the transition is a practically nonhysteretic weak first-order one, the hysteresis at T_I is hardly visible. In the case of the disorder appearing abruptly like at T_M , because the martensite is more disordered than the premartensitic phase, a residual resistivity jump takes place and, owing to the hysteretic nature of the first-order transition, the resistivity also exhibits a clear thermal hysteresis.

One might argue that the well-known mechanism of the electron density of states (DOS) redistribution near the Fermi level could also contribute to the $\rho(T)$ change at MT. We consider this assertion reasonable but the importance of this mechanism is still not clear.

TABLE I. Martensitic, T_M , and premartensitic, T_I , transition temperatures of Ni-Mn-Ga and Ni-Fe-Ga alloys obtained from resistivity curves under zero magnetic field. $(\partial T_{\text{af}}/\partial H)_{\text{exp}}$ is magnetic shift of martensitic transformation temperature T_{af} at high fields (Fig. 3). ΔM_{calc} is the calculated saturation magnetization jump at T_{af} . The Curie temperature, T_C , and transition heat, Q , are taken from Refs. 7, 8, 10, and 24–27.

Alloy	Composition	Martensite	T_M (K)	T_I (K)	T_C (K)	$(\partial T_{\text{af}}/\partial H)_{\text{exp}}$ (K/T)	$ Q $ (J/g)	ΔM_{calc} (A m ² /kg)
Ni51PC	Ni _{51.1} Mn _{24.9} Ga _{24.0}	10 M	190	250	378	0.26	1.4	1.75
Ni49SC	Ni _{49.5} Mn _{25.4} Ga _{25.1}	10 M	175	240	381	0.25	1.4	1.87
Fe19PC	Ni ₅₅ Fe ₁₉ Ga ₂₆	14 M	240		289	0.10	2.1	0.82
Fe20PC	Ni ₅₄ Fe ₂₀ Ga ₂₆	14 M	235		293	0.14	1.8	0.98
Fe21PC	Ni ₅₃ Fe ₂₁ Ga ₂₆	14 M	220		327	0.06	1.4	0.36

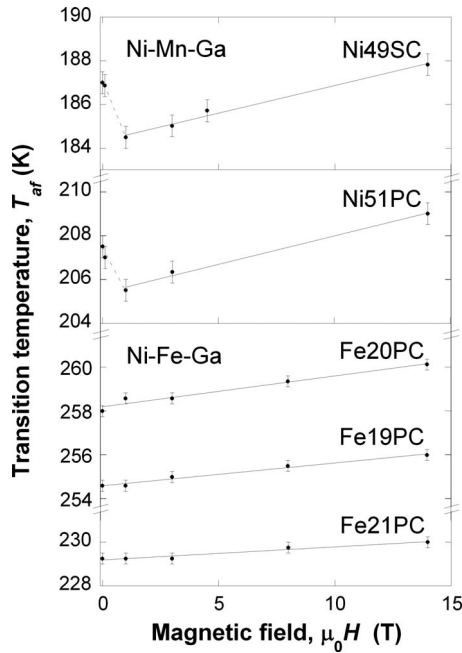


FIG. 3. Martensitic transformation temperatures as a function of magnetic field obtained from resistivity curves such as depicted in Figs. 1 and 2. A linear fit above the minimum is shown by the solid line.

B. Magnetic-field-induced shift of the transformation temperature

Under an applied magnetic field, the resistivity for all the alloys shifts monotonously downward due to the magnetoresistance and along the temperature axis reflecting the field dependence of the MT. The shift toward higher temperatures is monotonous for Ni-Fe-Ga alloys; both the polycrystalline and single crystalline Ni-Mn-Ga alloys demonstrate an initial tendency to lower temperatures. In order to quantify the shift of the MT under field, we selected the austenite finish temperature (T_{af}) determined by a tangential method, as shown by dashed lines and arrows in the insets of Figs. 1 and 2. This temperature, as well as the martensite start (T_{ms}), turned out to be defined within the minimal uncertainty bars shown in Fig. 3. The change in T_{af} is representative of the equilibrium temperature of the transformation (see, e.g., Ref. 34), therefore, we only refer to T_{af} , but all characteristic temperatures show the same variation. The T_{af} dependence is plotted in Fig. 3 for each alloy. From a thermodynamic point of view, the plots in Fig. 3 can be considered as quasiequilibrium T - H phase diagrams, similarly to the hydrostatic pressure and uniaxial stress phase diagrams of Ni-Mn-Ga alloys.^{14,18,20} In Fig. 3, T - H diagrams, for both single crystalline and polycrystalline Ni-Mn-Ga alloys, display a minimum at low magnetic field. Similar minima have been previously observed only in Ni-Mn-Ga single crystals.^{20,34} Figure 3 also confirms the shift of the MT under magnetic field for Ni-Fe-Ga alloys. This was not found before³³ probably due to instrumental limitations.

The straight solid lines shown in Fig. 3 are linear fits to the high magnetic-field data points. The slopes of these linear

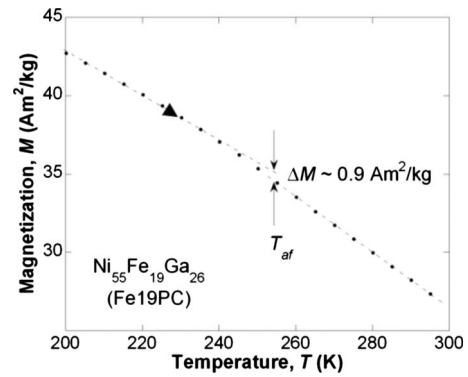


FIG. 4. Thermomagnetization heating curve of Fe19PC alloy measured in the saturating magnetic field of 2 T. A possible magnetization drop at the austenite transformation temperature is shown.

approximations are given in Table I. The values for the slopes of Ni51PC and Ni49SC alloys are the same within the error and agree with Ref. 34, whereas those for Ni-Fe-Ga alloys vary nonmonotonously with the composition.

The physical mechanisms of the magnetic-field effect on the MT in ferromagnetic shape memory alloys were considered in Refs. 18, 20, and 34–36. In saturating fields, i.e., above 1 T, the main contribution to the shift, $\partial T / \partial H$, is the magnetization change accompanying the transition, ΔM , as given by the Clausius-Clapeyron equation,

$$\frac{\partial T}{\partial H} = \frac{\Delta M}{\Delta S}, \quad (1)$$

where ΔS is the entropy change associated with the transition. Equation (1) can be used to obtain the values of ΔM as far as the other quantities are known. The results are presented in Table I. The uncertainties of the calculated ΔM values are within 10%, due to the uncertainty in the determination of the values of ΔS (about 5%) and the scatter in the T - H data. Theoretical studies show the importance of the ΔM because it reflects the Jahn-Teller band mechanism of the MT in ferromagnetic shape memory alloys. This takes place through the link of ΔM to both (a) the initial position of the Fermi level with regard to the peak of the density of states for the degenerate subband and (b) the exchange splitting of the spin subbands.³⁶ It is difficult to measure ΔM by conventional magnetic techniques, especially in polycrystals, due to its small magnitude and the smearing of the $M(T)$ anomaly at MT.²⁰ Figure 4 illustrates this difficulty, where only the previous knowledge of the MT temperature allows to identify ΔM . The value of ΔM shown in Fig. 4 is in a good agreement with the one calculated from Eq. (1) and displayed in Table I. Note that the decreasing value of ΔM in Ni-Fe-Ga alloys, when approaching the stoichiometric composition, is in line with the same findings in Ni-Mn-Ga alloys.²⁰

At low fields, i.e., below 1 T, a decrease in the MT temperature is observed for Ni-Mn-Ga alloys (Fig. 3). The transition temperature passes through a minimum before reaching the high-field linear behavior. A similar result was reported in Refs. 20 and 34 for single crystals and, recently,

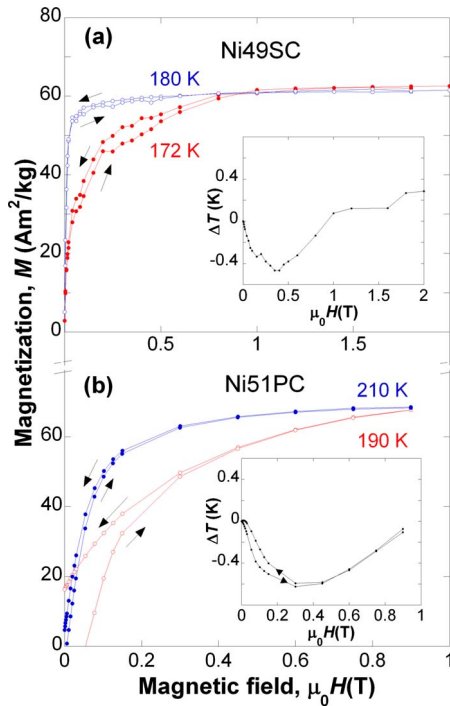


FIG. 5. (Color online) Magnetization curves of the premartensitic and martensitic phases in two Ni-Mn-Ga alloys. Insets depict magnetic shift of the martensitic transformation temperature, calculated by Eq. (1) and illustrating a low-field minimum.

also for the premartensitic transition.²⁹ The observed minimum was explained by using Eq. (1) and the different sign of ΔM at low field. Low-field values of ΔM arise because the magnetic anisotropy of the martensite is about one order of magnitude larger than in the austenite.^{29,34} To confirm this mechanism, Fig. 5 shows the magnetization of the intermediate and martensitic phases in the vicinity of the MT. Despite the difference in coercive fields between the two Ni-Mn-Ga alloys, they show main common features, such as similar values of the saturation field and a large difference in magnetic anisotropy between the intermediate and martensitic phases. This difference explains the negative ΔM in Eq. (1) and the appearance of the minimum in the $\Delta T-H$ curves, as calculated in the insets of Fig. 5.

For the Ni-Fe-Ga alloys the magnetization curves are very similar in the two phases, indicating a low magnetic anisotropy of the martensite. Therefore the minimum in $T-H$ diagram is not observed in this case.

C. Magnetoresistance

Magnetoresistance, and its relationship with the MT, is a technologically and physically sound phenomenon. It manifests as a monotonous shift of the resistivity under the magnetic field (Figs. 1 and 2). In Fig. 6, the zero-field resistivity curves for the Fe19PC alloy were subtracted from the nonzero-field ones. The magnetoresistance does not demonstrate a regular dependence on the phase state of the alloys. Instead, as a common feature, one can observe a steplike change and a minimum in the MR at the martensitic

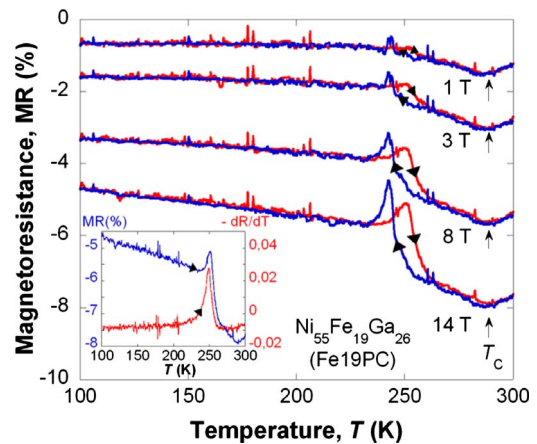


FIG. 6. (Color online) Heating-cooling longitudinal magnetoresistance under different constant magnetic fields for Ni-Fe-Ga alloy Fe19PC, obtained from the ramps in Fig. 2 by subtracting the zero-field curve and referred to the resistance value at 300 K. Data shown represent the typical behavior of all studied materials. The Curie temperature is indicated by the vertical arrows. The inset shows a comparison between the temperature dependence of magnetoresistance and the resistivity derivative at 14 T.

transition and a broad maximum at the Curie temperature. These anomalies increase their size as the magnetic field increases. The results in this alloy are shown in Fig. 6 as a prototypical example.

Three main mechanisms have been used to explain resistivity and MR in ferromagnets:^{11,37}

(i) domain or anisotropic magnetoresistance—this, however, saturates in low fields of the order of the anisotropy field;

(ii) intrinsic magnetic scattering, usually proportional to the square of the magnetization and always negative—this term increases with the temperature up to T_C , where it shows a maximum; and

(iii) interface spin scattering due to the different orientation of the magnetization at both sides of the interface—this term is also negative and saturates at low to moderate fields.

There are controversial explanations in the literature concerning the MR values in the martensitic and austenitic phases as well as about the peaks of MR appearing at the martensitic transformation. Most works^{12,13} tend to consider twin boundaries and interfaces as the main contribution to MR, i.e., mechanism (iii), but it has been directly found that the resistivity of a single crystal is not related to the number of twin boundaries present.³⁸ In our opinion there is an alternative and simple explanation of the MR features at the MT. In the vicinity of the martensitic transformation, one can approximate MR by the expression

$$\text{MR} \propto \frac{dR}{dH} \approx \frac{dR}{dT} \frac{dT}{dH}. \quad (2)$$

This shows that peak anomalies of MR are a combination of the resistivity change at MT and the magnetic-field-induced shift of the transformation temperature.

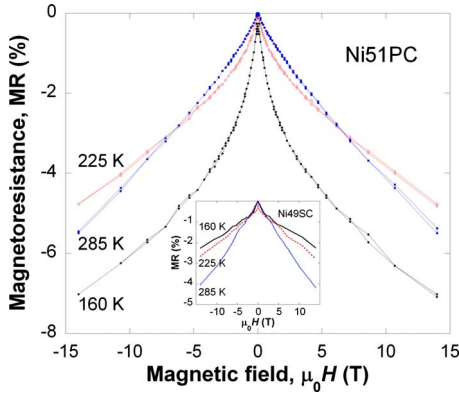


FIG. 7. (Color online) Longitudinal magnetoresistance versus magnetic field measured in three different phases of the polycrystalline Ni-Mn-Ga alloy, Ni51PC. The inset shows results for the single crystal Ni49SC.

The experimental results are in agreement with Eq. (2): (i) the correlation of MR with dR/dT is evidenced from the inset of Fig. 6; (ii) the correlation with the magnetic shift of the MT temperature is in line with the increase in the peak values in Fig. 6. Moreover Eq. (2) correctly predicts whether a maximum or minimum of the MR is expected to be observed at MT. “Classic” FSMAs, such as Ni-Mn-Ga, Ni-Fe-Ga, or Co-Ni-Ga, where both the martensite and austenite are ferromagnetic, must exhibit a minimum of MR, due to the positive value of dT/dH , as in Fig. 6 (see also Ref. 38). FSMAs, such as, Ni-Mn-Sn(In, Sb) with a huge Mn excess exhibiting a metamagnetic martensite and a ferromagnetic austenite (see, e.g., Ref. 39 and references therein) should display a maximum, due to the negative dT/dH value, as observed.⁴⁰ These effects also manifest during isothermal studies of the MR in the vicinity of the MT. The contemporary literature is rich in reports about “giant” magnetoresistance in FSMAs, in which the magnetic-field-induced MT takes place accompanied by a large resistivity change at the transition. The sharp enhancement or decrease in the MR takes place according to the mechanism described above.

Finally we have also measured the magnetoresistance in the different phases of the alloys. The results are shown in

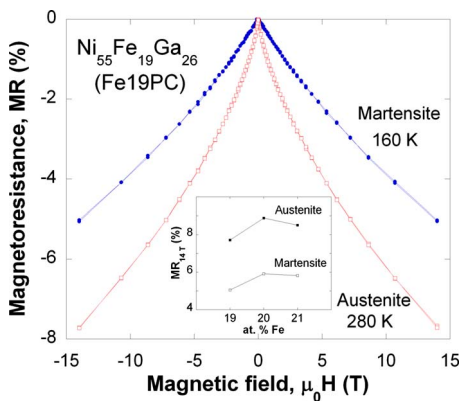


FIG. 8. (Color online) Longitudinal magnetoresistance of Fe19PC measured in the martensitic and austenitic phases. Displayed data are typical among Ni-Fe-Ga alloys. The inset shows the dependence of MR at 14 T on Fe concentration.

Figs. 7 and 8. They show fairly high values of negative MR, in agreement with data on Fig. 6, and also confirm our aforementioned assertion that there is no regularity in the values of MR in the different phases. In this respect, one should take with caution the conclusions in the literature drawn from the study of a single alloy composition (see, e.g., Refs. 12 and 13). For Ni51PC, MR in the martensitic phase is larger and much more nonlinear than in the austenite. The opposite is observed in the Ni49SC and Ni-Fe-Ga alloys. It is worth noting that the premartensitic phase can be distinguished by its peculiar MR behavior. Clearly, the spin disorder scattering is larger in the cubic phase than in the modulated premartensitic phase in both Ni-Mn-Ga alloys (Fig. 7). The lowest values of MR for the Ni49SC alloy suggest its magnetically more homogeneous state, as compared with the polycrystalline one. From Fig. 6 and Table I, it can be deduced that the main reason for the largest MR of the Ni-Fe-Ga alloys taking place in austenite (at $T=290$ K) is the close proximity to the Curie temperature. The evolution of the MR as a function of Fe concentration (inset of Fig. 8) can be related to the interplay between the formation of magnetic inhomogeneities (clusters) and the ferromagnetic γ -phase precipitates formed during annealing.

According to the data in Figs. 7 and 8, our results can be attributed to the mechanism (ii) mentioned before. That means that the Heusler alloys studied, even in single crystalline form, are magnetically inhomogeneous, as they can contain, e.g., antiferromagnetic clusters of Mn atoms. The structural transition of the ferromagnetic matrix can modify the local magnetic disorder, largely due to technological factors such as melting, casting, annealing, etc. The type and degree of local disorder are unique for each alloy and *a priori* hardly predictable. Note that any effect of partial martensite transformation that could give a mixture of both phases at low temperature was ruled out in the present work by careful x-ray and neutron diffraction experiments that demonstrate a complete transformation,^{7,10} except for the γ phases present in FeNiGa alloys.

IV. CONCLUSIONS

In summary, we have measured the martensitic transformation temperature versus magnetic-field phase diagrams for the single crystalline and polycrystalline Ni-Mn-Ga and Ni-Fe-Ga FSMAs by accurately measuring the resistivity as a function of temperature and magnetic field. At low field, a minimum in T_M is found in the case of Ni-Mn-Ga alloys. This minimum is attributed to the magnetic anisotropy contribution to the Clausius-Clapeyron equation and confirmed by direct magnetization measurements in the two phases. Ni-Fe-Ga alloys do not show any minimum due to the small difference in magnetic anisotropies between the two phases involved. An analysis of the magnetoresistance in FSMAs made possible to clarify the origin of the peak values of the MR at the MT as well as to assign the mechanism responsible for MR. The estimated values of ΔM that characterize the MT can be used to tackle the general problem of the magnetic-field influence on the Jahn-Teller band effect in the conducting ferromagnets.

ACKNOWLEDGMENTS

The financial support from the Department of Education, Basque Government (Project No. IT-347-07) and the Spanish Ministry of Education and Science (Project No. MAT2008-

06542-C04-02) is acknowledged. J.F. is grateful to the EC Marie Curie IIF Initiative under Grant No. FP6. University general services (SGIker) Chief Engineer of Magnetic Measurements, I. Orúe, is acknowledged for the delicate resistivity and MR measurements.

*Author to whom correspondence should be addressed; manub@we.lc.ehu.es

- ¹*Shape Memory Materials*, edited by K. Otsuka and C. M. Wayman (Cambridge University Press, Cambridge, 1998).
- ²*Advances in Shape Memory Materials*, edited by V. A. Chernenko (TTP, Zurich, Switzerland, 2008), Vol. 583.
- ³A. Sozinov, A. A. Likhachev, and K. Ullakko, *IEEE Trans. Magn.* **38**, 2814 (2002).
- ⁴P. Müllner, V. A. Chernenko, and G. Kostorz, *J. Appl. Phys.* **95**, 1531 (2004).
- ⁵Z. H. Liu, M. Zhang, Y. T. Cui, Y. Q. Zhou, W. H. Wang, G. H. Wu, X. X. Zhang, and G. Xiao, *Appl. Phys. Lett.* **82**, 424 (2003).
- ⁶T. Omori, N. Kamiya, Y. Sutou, K. Oikawa, R. Kainuma, and K. Ishida, *Mater. Sci. Eng., A* **378**, 403 (2004).
- ⁷J. Gutiérrez, P. Lazpita, V. Siruguri, J. M. Barandiaran, P. Henry, V. A. Chernenko, and T. Kanomata, *Int. J. Appl. Electromagn. Mech.* **23**, 71 (2006).
- ⁸V. A. Chernenko, *Scr. Mater.* **40**, 523 (1999).
- ⁹F. Zuo, X. Su, P. Zhang, G. C. Alexandrakis, F. Yang, and K. H. Wu, *J. Phys.: Condens. Matter* **11**, 2821 (1999).
- ¹⁰M. Barandiaran, J. Gutiérrez, P. Lazpita, V. A. Chernenko, C. Seguí, J. Pons, E. Cesari, K. Oikawa, and T. Kanomata, *Mater. Sci. Eng., A* **478**, 125 (2008).
- ¹¹V. O. Golub, A. Y. Vovk, L. Malkinski, C. J. O'Connor, Z. Wang, and J. Tang, *J. Appl. Phys.* **96**, 3865 (2004).
- ¹²Z. H. Liu, H. Liu, X. X. Zhang, X. K. Zhang, J. Q. Xiao, Z. Y. Zhu, X. F. Dai, G. D. Liu, J. L. Chen, and G. H. Wu, *Appl. Phys. Lett.* **86**, 182507 (2005).
- ¹³C. Biswas, R. Rawat, and S. R. Barman, *Appl. Phys. Lett.* **86**, 202508 (2005).
- ¹⁴J. Kim, F. Inaba, T. Fukuda, and T. Kakeshita, *Acta Mater.* **54**, 493 (2006).
- ¹⁵C. Seguí, V. A. Chernenko, J. Pons, E. Cesari, V. Khovailo, and T. Takagi, *Acta Mater.* **53**, 111 (2005).
- ¹⁶F. Zuo, X. Su, and K. H. Wu, *Phys. Rev. B* **58**, 11127 (1998).
- ¹⁷W. H. Wang, J. L. Chen, S. X. Gao, G. H. Wu, Z. Wang, Y. F. Zheng, L. C. Zhao, and W. S. Zhan, *J. Phys.: Condens. Matter* **13**, 2607 (2001).
- ¹⁸V. A. Chernenko, O. Babii, V. L'vov, and P. G. McCormick, *Mater. Sci. Forum* **327&328**, 485 (2000).
- ¹⁹V. V. Khovailo, V. Novosad, T. Takagi, D. A. Filippov, R. Z. Levitin, and A. N. Vasil'ev, *Phys. Rev. B* **70**, 174413 (2004).
- ²⁰V. A. Chernenko, V. A. L'vov, T. Kanomata, T. Kakeshita, K. Koyama, and S. Besseghini, *Mater. Trans.* **47**, 635 (2006).
- ²¹Y. T. Cui, J. L. Chen, G. D. Liu, G. H. Wu, and W. L. Wang, *J. Phys.: Condens. Matter* **16**, 3061 (2004).
- ²²Y. Ma, S. Awaji, K. Watanabe, M. Matsumoto, and N. Kobayashi, *Appl. Phys. Lett.* **76**, 37 (2000).
- ²³A. Gonzalez-Comas, E. Obrado, L. Manosa, A. Planes, V. A. Chernenko, B. J. Hattink, and A. Labarta, *Phys. Rev. B* **60**, 7085 (1999).
- ²⁴V. A. Chernenko, J. Pons, C. Seguí, and E. Cesari, *Acta Mater.* **50**, 53 (2002).
- ²⁵J. Gutiérrez, P. Lázpita, J. M. Barandiarán, J. S. Garitaonandia, F. Plazaola, E. Legarra, V. A. Chernenko, and T. Kanomata, *Hyperfine Interact.* **168**, 1207 (2006).
- ²⁶G. Fritsch, V. V. Kokorin, V. A. Chernenko, A. Kempf, and I. K. Zasmichuk, *Phase Transitions* **57**, 233 (1996).
- ²⁷J. Pons, V. A. Chernenko, R. Santamarta, and E. Cesari, *Acta Mater.* **48**, 3027 (2000).
- ²⁸Y. Zhou, X. Jin, H. Xu, Y. V. Kudryavtsev, Y. P. Lee, and J. Y. Rhee, *J. Appl. Phys.* **91**, 9894 (2002).
- ²⁹J. M. Barandiaran, V. A. Chernenko, P. Lazpita, J. Gutiérrez, I. Orue, J. Feuchtwanger, and S. Besseghini, *Appl. Phys. Lett.* **94**, 051909 (2009).
- ³⁰J. I. Pérez-Landazábal, V. Sánchez-Alarcos, C. Gómez-Polo, V. Recarte, and V. A. Chernenko, *Phys. Rev. B* **76**, 092101 (2007).
- ³¹V. A. Chernenko, A. Fujita, S. Besseghini, and J. I. Pérez-Landazábal, *J. Magn. Magn. Mater.* **320**, e156 (2008).
- ³²V. A. Chernenko, V. A. L'vov, S. P. Zagorodnyuk, and T. Takagi, *Phys. Rev. B* **67**, 064407 (2003).
- ³³O. Heczko, S. Fähler, T. M. Vasilchikova, T. N. Voloshok, K. V. Klimov, Yu. I. Chumlyakov, and A. N. Vasiliev, *Phys. Rev. B* **77**, 174402 (2008).
- ³⁴T. Fukuda and T. Kakeshita, *Adv. Mater. Res.* **52**, 199 (2008).
- ³⁵K. Shimizu, N. Yamano, T. Kakeshita, M. Ono, K. Sugiyama, and M. Date, *Mater. Sci. Forum* **56-58**, 235 (1990).
- ³⁶A. F. Popkov, A. I. Popov, A. V. Goryachev, and V. G. Shavrov, *Sov. Phys. JETP* **104**, 943 (2007).
- ³⁷P. L. Rossiter, *The Electrical Resistivity of Metals and Alloys* (Cambridge University Press, Cambridge, 1987).
- ³⁸V. K. Srivastava, R. Chatterjee, and R. C. O'Handley, *Appl. Phys. Lett.* **89**, 222107 (2006).
- ³⁹S. Y. Yu, L. Ma, G. D. Liu, Z. H. Liu, J. L. Chen, Z. X. Cao, G. H. Wu, B. Zhang, and X. X. Zhang, *Appl. Phys. Lett.* **90**, 242501 (2007).
- ⁴⁰M. Khan, I. Dubenko, S. Stadler, and N. Ali, *J. Phys.: Condens. Matter* **20**, 235204 (2008).